Monthly Notices
of the
ROYAL ASTRONOMICAL SOCIETY

MNRAS **459,** 487–495 (2016)
Advance Access publication 2016 March 23

doi:10.1093/mnras/stw676

GRACES observations of young [α/Fe]-rich stars

David Yong,[1]★ Luca Casagrande,[1] Kim A. Venn,[2] André-Nicolas Chené,[3] Jared Keown,[2] Lison Malo,[4] Eder Martioli,[5] Alan Alves-Brito,[6] Martin Asplund,[1] Aaron Dotter,[1] Sarah L. Martell,[7] Jorge Meléndez[8] and Katharine J. Schlesinger[1]

[1]*Research School of Astronomy and Astrophysics, Australian National University, Canberra, ACT 2611, Australia*
[2]*Department of Physics and Astronomy, University of Victoria, Victoria, BC V8W 3P2, Canada*
[3]*Gemini Observatory, Northern Operations Centre, 670 North A'ohoku Place, Hilo, HI 96720, USA*
[4]*Canada–France–Hawaii Telescope Corporation, 65-1238 Mamalahoa Highway, Kamuela, HI 96743, USA*
[5]*Laboratório Nacional de Astrofísica (LNA/MCTI), Rua Estados Unidos, 154, Itajubá, MG, Brazil*
[6]*Instituto de Fisica, Universidade Federal do Rio Grande do Sul, Av. Bento Goncalves 9500, Porto Alegre, RS, Brazil*
[7]*School of Physics, University of New South Wales, Sydney, NSW 2052, Australia*
[8]*Departamento de Astronomia do IAG/USP, Universidade de São Paulo, Rua do Matão 1226, Cidade Universitária, 05508-900 São Paulo, SP, Brazil*

Accepted 2016 March 18. Received 2016 March 18; in original form 2015 November 18

ABSTRACT

We measure chemical abundance ratios and radial velocities in four massive (i.e. young) [α/Fe]-rich red giant stars using high-resolution high-S/N spectra from ESPaDOnS fed by Gemini-GRACES. Our differential analysis ensures that our chemical abundances are on the same scale as the Alves-Brito et al. (2010) study of bulge, thin, and thick disc red giants. We confirm that the program stars have enhanced [α/Fe] ratios and are slightly metal poor. Aside from lithium enrichment in one object, the program stars exhibit no chemical abundance anomalies when compared to giant stars of similar metallicity throughout the Galaxy. This includes the elements Li, O, Si, Ca, Ti, Cr, Ni, Cu, Ba, La, and Eu. Therefore, there are no obvious chemical signatures that can help to reveal the origin of these unusual stars. While our new observations show that only one star (not the Li-rich object) exhibits a radial velocity variation, simulations indicate that we cannot exclude the possibility that all four could be binaries. In addition, we find that two (possibly three) stars show evidence for an infrared excess, indicative of a debris disc. This is consistent with these young [α/Fe]-rich stars being evolved blue stragglers, suggesting their apparent young age is a consequence of a merger or mass transfer. We would expect a binary fraction of ∼50 per cent or greater for the entire sample of these stars, but the signs of the circumbinary disc may have been lost since these features can have short time-scales. Radial velocity monitoring is needed to confirm the blue straggler origin.

Key words: techniques: radial velocities – stars: abundances.

1 INTRODUCTION

The atmospheres of low-mass stars retain, to a large extent, detailed information on the chemical composition of the interstellar medium at the time and place of their birth. The chemical abundance ratio [α/Fe] has long served as a key indicator of the relative contributions of different types of stars and thus the degree of chemical enrichment (e.g. Tinsley 1979; Matteucci & Greggio 1986; Venn et al. 2004). Massive stars with short lifetimes that die as core collapse supernovae (SNe II) produce α-elements and modest amounts of Fe whereas longer lived thermonuclear supernovae (SNe Ia) dominate the production of Fe-peak elements. Enhanced [α/Fe] ratios therefore indicate that the stars are relatively old such that the gas from which they formed included SNe II contributions, but not those from SNe Ia. Indeed, stars with high [α/Fe] ratios are generally older than ∼8 Gyr (e.g. Fuhrmann 2011; Bensby, Feltzing & Oey 2014).

Asteroseismology from the *CoRoT* (Baglin et al. 2006) and *Kepler* (Gilliland et al. 2010) satellite missions have enabled accurate measurements of stellar masses and radii based on standard seismic scaling relations for stars with solar-like oscillations (Ulrich 1986; Brown et al. 1991; Chaplin & Miglio 2013). Those mass determinations greatly help to derive more robust age estimates

★ E-mail: yong@mso.anu.edu.au

Table 1. Details of the observations.

2MASS ID	Filename	OBSID	Date/UT at end	Exptime (s)	Airmass	Instrument mode
J19081716+3924583	N20150604G0033.fits	GN-2015A-SV-171-9	2015-06-04/08:41:38	180	2.03	Spectroscopy, star only
J19081716+3924583	N20150604G0034.fits	GN-2015A-SV-171-9	2015-06-04/08:45:42	180	2.11	Spectroscopy, star only
J19081716+3924583	N20150604G0035.fits	GN-2015A-SV-171-9	2015-06-04/08:49:53	180	2.06	Spectroscopy, star only
J19093999+4913392	N20150721G0045.fits	GN-2015A-SV-171-11	2015-07-21/09:56:48	180	1.16	Spectroscopy, star only
J19093999+4913392	N20150721G0046.fits	GN-2015A-SV-171-11	2015-07-21/10:00:40	180	1.15	Spectroscopy, star only
J19093999+4913392	N20150721G0047.fits	GN-2015A-SV-171-11	2015-07-21/10:04:32	180	1.15	Spectroscopy, star only
J19083615+4641212	N20150721G0049.fits	GN-2015A-SV-171-13	2015-07-21/10:24:40	180	1.14	Spectroscopy, star only
J19083615+4641212	N20150721G0050.fits	GN-2015A-SV-171-13	2015-07-21/10:28:31	180	1.14	Spectroscopy, star only
J19083615+4641212	N20150721G0051.fits	GN-2015A-SV-171-13	2015-07-21/10:32:23	180	1.15	Spectroscopy, star only
J19101154+3915484	N20150721G0052.fits	GN-2015A-SV-171-15	2015-07-21/10:43:59	180	1.10	Spectroscopy, star only
J19101154+3915484	N20150721G0053.fits	GN-2015A-SV-171-15	2015-07-21/10:47:50	180	1.10	Spectroscopy, star only
J19101154+3915484	N20150721G0054.fits	GN-2015A-SV-171-15	2015-07-21/10:51:43	180	1.10	Spectroscopy, star only

(e.g. Silva Aguirre et al. 2013, 2015; Chaplin et al. 2014; Lebreton & Goupil 2014). For red giants in particular, their ages are determined to good approximation by the time spent in the hydrogen burning phase, which is predominantly a function of mass (e.g. Miglio et al. 2013b; Casagrande et al. 2015). The combination of chemical abundance measurements and asteroseismic information has broadly confirmed that stars with higher overall metallicity, [Fe/H], and solar [α/Fe] ratios are young whereas stars with lower metallicity and higher [α/Fe] ratios are old. Additionally, Nissen (2015) showed a strong correlation between [α/Fe] and isochrone-based ages among thin disc stars, with the oldest stars having the highest [α/Fe] ratios.

A challenge to this general picture has emerged through the discovery of a handful of stars with enhanced [α/Fe] ratios and high masses that result in young inferred ages (Chiappini et al. 2015; Martig et al. 2015). Martig et al. (2015) identified a sample of 14 stars younger than 6 Gyr with [α/Fe] $\geq +0.13$ based on high-resolution infrared (IR) spectra from Apache Point Observatory Galactic Evolution Experiment (APOGEE; Majewski et al. 2015). These unusually high masses ($M \gtrsim 1.4$ M$_\odot$), and thus young ages, are robust to modifications to the standard seismic scaling relations and to the assumption that the helium mass fractions are low (i.e. primordial). While Epstein et al. (2014) examined potential issues in the scaling relations for metal-poor stars with [Fe/H] < -1, Martig et al. (2015) dismissed this possibility (see section 7 in their paper) and existing tests for red giant stars indicate that the masses are likely accurate to better than $\sim$10 per cent (Miglio et al. 2013a). The spatial distributions, radial velocities and guiding radii for the young α-rich stars are indistinguishable from the α-rich population. Definitive population membership, based on kinematics, is currently limited by the proper-motion uncertainties.

Possible explanations for the origin of these stars include (i) they are evolved blue stragglers whose current masses lead to spurious age determinations, (ii) they were formed during a recent gas accretion episode in the Milky Way, or (iii) they were born near the corotation radius near the Galactic bar (Chiappini et al. 2015; Martig et al. 2015). For the former explanation, increasing the mass of a red giant from $\sim$1.0 to $\sim$1.4 M$_\odot$ would lower the inferred age by about 5 Gyr (Dotter et al. 2008), and that amount of material is consistent with blue straggler formation scenarios (Sills, Karakas & Lattanzio 2009). For the latter two explanations, the basic premise is that the stars are genuinely young and that the gas from which they formed remained relatively unprocessed reflecting mainly SNe II ejecta. Numerical simulations with inhomogeneous chemical enrichment predict a small fraction of young stars ($\sim$ 3 Gyr) with high [α/Fe] ratios (Kobayashi & Nakasato 2011) and young metal-rich stars with high [α/Fe] ratios have been observed in the Galactic Centre (Cunha et al. 2007).

The goal of this work is to confirm the [α/Fe] ratios of four young stars from Martig et al. (2015), identify any chemical signature that may provide clues to the origin of these objects and measure radial velocities to better understand the binary fraction.

2 SAMPLE SELECTION, OBSERVATIONS, AND ANALYSIS

The sample consists of four stars with [α/Fe] $\geq +0.20$ and ages < 4.0 Gyr from Martig et al. (2015), see Tables 1 and 2. High resolution ($R = 67{,}500$), high signal-to-noise ratio (S/N $\simeq$ 150–300 per pixel near 6500 Å) optical spectra were taken during initial science observations using the Gemini Remote Access to CFHT ESPaDOnS (Donati 2003) Spectrograph (GRACES; Chené et al. 2014) in 2015 June and July using the 1-fibre mode. Briefly, light from the Gemini North telescope is fed to the Echelle SpectroPolarimetric Device for the Observation of Stars (ESPaDOnS) at the Canada–France–Hawaii Telescope (CFHT) via two 270 m long optical fibres with $\sim$8 per cent throughput (see Chené et al. 2014). Details of the observations are provided in Table 1. Data reduction was performed using the OPERA pipeline (Martioli et al. 2012, Malo et al., in preparation) and reduced spectra are available from the Gemini web site (http://www.gemini.edu/sciops/instruments/july-2015-onsky-tests). Subsequent to those data being made publicly available, the OPERA pipeline was updated by LM and the spectra were re-reduced.[1] We used the unnormalized spectra without automatic correction of the wavelength solution using telluric lines and co-added the individual exposures for a given star. Continuum normalization was performed using routines in IRAF.[2]

The effective temperatures ($T_{\rm eff}$) for the program stars were determined using the IR flux method following Casagrande et al. (2010, 2014). The surface gravity ($\log g$) was determined from the masses and radii obtained using the standard seismic scaling relations, and our $\log g$ values are essentially identical to those of Pinsonneault

[1] Our results and conclusions are unchanged whether we use the publicly available or re-reduced spectra.

[2] IRAF is distributed by the National Optical Astronomy Observatories, which are operated by the Association of Universities for Research in Astronomy, Inc., under cooperative agreement with the National Science Foundation.

Table 2. Stellar parameters.

KIC ID	2MASS ID	$T_{\rm eff}$ (K)	log g (cgs)	ξ_t (km s^{-1})	[Fe/H] (dex)	Mass[a] ($M_\odot$)	Age[a] (Gyr)
4350501	J19081716+3924583	4689	3.05	1.01	−0.14	1.65 ± 0.20	<3.0
9821622	J19083615+4641212	4895	2.71	1.18	−0.40	1.71 ± 0.26	<2.6
11394905	J19093999+4913392	4951	2.50	1.38	−0.51	1.40 ± 0.18	<4.0
4143460	J19101154+3914584	4711	2.50	1.26	−0.39	1.58 ± 0.20	<3.1
			Comparison field giant				
HD 40409	J05540606−6305230	4746	3.20	1.19	+0.22	–	–

Note. [a]These values are taken directly from Martig et al. (2015). The masses are from the scaling relations.

Table 3. Line list for the program stars. This table is published in its entirety in the electronic edition of the paper. A portion is shown here for guidance regarding its form and content.

Wavelength (Å) (1)	Species[a] (2)	L.E.P (eV) (3)	log gf (4)	KIC 4350501 (mÅ) (5)	KIC 9821622 (mÅ) (6)	KIC 11394905 (mÅ) (7)	KIC 4143460 (mÅ) (8)	HD 40409 (mÅ) (9)	Source[b] (10)
6300.31	8.0	0.00	−9.75			Spectrum synthesis			B
7771.95	8.0	9.15	0.35	38.5	39.2	–	45.6	29.4	B
7774.18	8.0	9.15	0.21	38.0	30.6	39.3	43.6	33.9	B
5665.56	14.0	4.92	−2.04	56.0	48.7	46.3	57.4	67.5	B
5684.49	14.0	4.95	−1.65	69.2	–	–	–	–	B

Notes. [a]The digits to the left of the decimal point are the atomic number. The digit to the right of the decimal point is the ionization state ('0' = neutral, '1' = singly ionized).
[b]A = log gf values used in Yong et al. (2005) where the references include Ivans et al. (2001), Kurucz & Bell (1995), Prochaska et al. (2000), and Ramírez & Cohen (2002); B = Gratton et al. (2003); C = Oxford group including Blackwell et al. (1979a), Blackwell, Petford & Shallis (1979b), Blackwell et al. (1980, 1986), and Blackwell, Lynas-Gray & Smith (1995); D = Fuhr & Wiese (2006), using line component patterns for hfs/IS from Kurucz & Bell (1995); E = Fuhr & Wiese (2006), using hfs/IS from McWilliam (1998); F = Lawler, Bonvallet & Sneden (2001a), using hfs from Ivans et al. (2006); G = Lawler et al. (2001b), using hfs/IS from Ivans et al. (2006).

et al. (2014); the average difference in log g was 0.010 ± 0.007 (σ = 0.013). Equivalent widths (EWs) were measured by fitting Gaussian functions using routines in IRAF and DAOSPEC (Stetson & Pancino 2008). The two sets of EW measurements were in excellent agreement (<IRAF − DAOSPEC> = 0.8 mÅ; σ = 1.6 mÅ) and were averaged (see Table 3). (The minimum and maximum EWs used in the analysis were 7 mÅ and 125 mÅ, respectively.) Chemical abundances were obtained using the local thermodynamic equilibrium (LTE) stellar line analysis program MOOG (Sneden 1973; Sobeck et al. 2011) and one-dimensional LTE model atmospheres with [α/Fe] = +0.4 from Castelli & Kurucz (2003). The microturbulent velocity (ξ_t) was estimated by forcing no trend between the abundance from Fe I lines and the reduced EW. We required that the derived metallicity be within 0.1 dex of the value adopted in the model atmosphere. The final stellar parameters are presented in Table 2. We estimate that the internal uncertainties in $T_{\rm eff}$, log g, and ξ_t are 50 K, 0.05 cgs, and 0.2 km s^{-1}, respectively. Our stellar parameters are in good agreement with the values published in Martig et al. (2015); the average differences in $T_{\rm eff}$, log g, and [Fe/H] are 2 ± 66 K, −0.04 ± 0.05 cgs, and −0.09 ± 0.02 dex, respectively.

Chemical abundances for other elements were obtained using the measured EWs, final model atmospheres and MOOG. For the 6300 Å [O I] line, Cu and the neutron-capture elements, abundances were determined via spectrum synthesis and χ^2 minimization. For the 6300 Å [O I] line, our line list includes the Ni blend (which only contributes <20 per cent to the total EW). The abundances from the 6300 Å [O I] line are, on average, lower than the abundances from the 777nm O triplet by ∼ 0.3 dex. That difference is in good agreement with the non-local thermodynamic equilibrium (NLTE) corrections by Amarsi et al. (2015) (when assuming $A(O)_{LTE} = 8.8$, $T_{\rm eff}$ = 5000 K, log g = 3.0, and [Fe/H] = −0.5; their grid does not yet extend to lower $T_{\rm eff}$ and lower log g). For Cu, Ba, La, and Eu, we included isotopic shifts (IS) assuming solar abundances and hyperfine structure (hfs) in the line lists. The chemical abundances are presented in Tables 4 and 5. We adopted solar abundances from Asplund et al. (2009) and the uncertainties were determined following the approach in Yong et al. (2014). The abundance uncertainties from errors in the stellar parameters are provided in Table 6. For the majority of lines, we used damping constants from Barklem, Piskunov & O'Mara (2000) and Barklem & Aspelund-Johansson (2005). For the remaining lines, we used the Unsöld (1955) approximation.

A bright comparison giant star (HD 40409) studied by Alves-Brito et al. (2010) was also included in our analysis. After comparing our abundance ratios with those of Alves-Brito et al. (2010) for the comparison star HD 40409,[3] we made minor offsets[4] to place our Fe and α-element abundances on to their scale to aid our interpretation in the following sections; Alves-Brito et al. did not report abundances for the other elements.

We re-analysed the stars using ATLAS9 model atmospheres generated by Mészáros et al. (2012). When compared to the ATLAS9 models by Kurucz (1993) and Castelli & Kurucz (2003), the newer models include an updated H_2O line list, a larger range of carbon and α-element abundances and solar abundances from Asplund

[3] Stellar parameters for the comparison star were taken from Alves-Brito et al. (2010) as we were unable to apply the same methods as for the program stars.
[4] The average offset was −0.06 and the individual values were: Fe I (+0.01), Fe II (−0.15), O I (−0.17), Si I (−0.18), Ca I (+0.11), and Ti I (+0.04). For Fe II, O I, and Si I, the differences are non-negligible and likely due to differences in the line selection and atomic data.

Table 4. Chemical abundances for the program stars (O I–Fe II).

Name	A(X)	N_{lines}	s.e.$_{\log\epsilon}$	[X/Fe]	σ[X/Fe]
		O I			
KIC 4350501	9.07	3	0.05	0.53	0.16
KIC 9821622	8.40	3	0.08	0.11	0.13
KIC 11394905	8.24	2	0.10	0.07	0.15
KIC 4143460	8.90	2	0.03	0.60	0.14
HD 40409	9.01	2	0.14	0.10	0.17
		Si I			
KIC 4350501	7.55	16	0.02	0.18	0.06
KIC 9821622	7.17	15	0.02	0.06	0.07
KIC 11394905	7.05	13	0.03	0.05	0.06
KIC 4143460	7.30	12	0.03	0.18	0.06
HD 40409	7.74	10	0.05	0.01	0.07
		Ca I			
KIC 4350501	6.23	9	0.04	0.04	0.07
KIC 9821622	6.30	10	0.03	0.36	0.06
KIC 11394905	6.09	9	0.03	0.27	0.06
KIC 4143460	6.20	10	0.03	0.25	0.08
HD 40409	6.47	3	0.03	−0.09	0.10
		Ti I			
KIC 4350501	4.83	25	0.02	0.02	0.07
KIC 9821622	4.95	33	0.02	0.40	0.06
KIC 11394905	4.73	20	0.02	0.29	0.05
KIC 4143460	4.75	23	0.02	0.19	0.07
HD 40409	5.14	19	0.03	−0.03	0.08
		Cr I			
KIC 4350501	5.39	8	0.07	−0.10	0.08
KIC 9821622	5.31	7	0.06	0.07	0.06
KIC 11394905	5.17	7	0.06	0.05	0.06
KIC 4143460	5.25	6	0.08	0.00	0.09
HD 40409	5.77	5	0.09	−0.09	0.10
		Fe I			
KIC 4350501	7.34	98	0.01	−0.16	0.08
KIC 9821622	7.12	98	0.01	−0.38	0.07
KIC 11394905	7.00	99	0.01	−0.50	0.07
KIC 4143460	7.11	87	0.01	−0.39	0.08
HD 40409	7.71	58	0.01	0.21	0.09
		Fe II			
KIC 4350501	7.50	10	0.04	0.00	0.11
KIC 9821622	6.93	10	0.03	−0.57	0.10
KIC 11394905	6.81	8	0.03	−0.69	0.11
KIC 4143460	7.12	12	0.03	−0.38	0.11
HD 40409	7.80	6	0.04	0.30	0.12

Table 5. Chemical abundances for the program stars (Ni I–Eu II).

Name	A(X)	N_{lines}	s.e.$_{\log\epsilon}$	[X/Fe]	σ[X/Fe]
		Ni I			
KIC 4350501	6.14	23	0.02	0.06	0.03
KIC 9821622	5.86	19	0.01	0.04	0.04
KIC 11394905	5.70	19	0.01	−0.01	0.04
KIC 4143460	5.86	23	0.02	0.03	0.03
HD 40409	6.47	18	0.02	0.03	0.04
		Cu I			
KIC 4350501	4.08	2	0.09	0.03	0.12
KIC 9821622	3.71	2	0.12	−0.09	0.13
KIC 11394905	3.57	2	0.09	−0.11	0.15
KIC 4143460	3.71	2	0.07	−0.08	0.12
HD 40409	4.38	2	0.06	−0.03	0.11
		Ba II			
KIC 4350501	2.06	3	0.12	0.02	0.13
KIC 9821622	1.83	3	0.11	0.04	0.16
KIC 11394905	1.80	3	0.08	0.14	0.15
KIC 4143460	1.91	3	0.14	0.12	0.18
HD 40409	2.42	3	0.13	0.02	0.15
		La II			
KIC 4350501	1.01	2	0.06	0.05	0.11
KIC 9821622	0.88	2	0.10	0.18	0.11
KIC 11394905	0.82	2	0.12	0.24	0.14
KIC 4143460	0.94	2	0.04	0.23	0.12
HD 40409	1.57	2	0.03	0.25	0.12
		Eu II			
KIC 4350501	0.74	1	–	0.36	0.16
KIC 9821622	0.66	1	–	0.54	0.16
KIC 11394905	0.47	1	–	0.46	0.17
KIC 4143460	0.64	1	–	0.51	0.16
HD 40409	0.73	1	–	−0.01	0.16

Table 6. Abundance errors from uncertainties in atmospheric parameters. This table is published in its entirety in the electronic edition of the paper. A portion is shown here for guidance regarding its form and content.

Species	$\Delta T_{\rm eff}$ +50 K	$\Delta\log g$ +0.05 cgs	$\Delta\xi_t$ +0.2 km s^{-1}	Δ[m/H] +0.2 dex	Total[a]
			KIC 4350501		
Δ[O I/Fe]	−0.10	0.04	0.06	−0.04	0.13
Δ[Si I/Fe]	−0.03	0.01	0.04	−0.00	0.05
Δ[Ca I/Fe]	0.05	−0.01	−0.01	−0.01	0.05
Δ[Ti I/Fe]	0.06	−0.01	0.02	−0.01	0.06
Δ[Cr I/Fe]	0.04	−0.01	0.01	−0.01	0.04

Note. [a]The total error is determined by adding in quadrature the first four entries.

et al. (2009). The average difference in [X/Fe] ratios [Mészáros et al. 2012 (with [C/Fe] = 0 and [α/Fe] = +0.3) − Castelli & Kurucz 2003 was only −0.03 ± 0.01 dex.

3 RESULTS

We confirm that the program stars are slightly more metal poor than the Sun and have enhanced [α/Fe] ratios (α is the average of O, Si, Ca, and Ti). That is, our independent study using optical spectra from GRACES largely confirms the results from the APOGEE pipeline analysis of the IR *H*-band spectrum (García Pérez et al. 2015; Majewski et al. 2015).

Examination of the individual α-elements (O, Si, Ca, and Ti), however, reveals subtle differences among those elements (see Fig. 1). For O and Si, the two most metal-rich stars have higher [X/Fe] ratios when compared to the two most metal-poor stars. For Ca and Ti, however, the situation is reversed in that the two most metal-rich stars have lower [X/Fe] ratios. And therefore on average, all stars have similar [α/Fe] ratios.

Fig. 1 enables us to compare the abundance ratios of the program stars with the thin disc, thick disc, and bulge red giant stars from Alves-Brito et al. (2010).[5] Recall that our analysis includes HD 40409 also studied by Alves-Brito et al. (2010) and that we have adjusted our abundance scale to match theirs (at least for Fe and the α-elements). Therefore, we are confident that there are no major systematic abundance offsets between the program stars and the

[5] The main conclusion of that work was that the bulge and local thick disc stars are chemically similar and that they are distinct from the local thin disc.

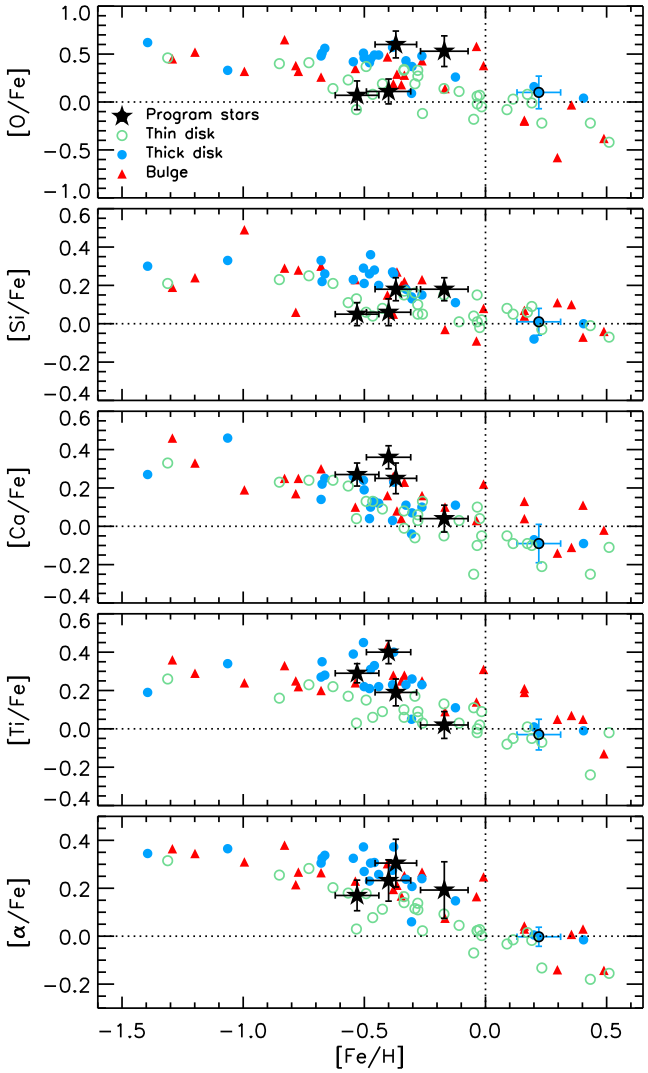

Figure 1. Abundance [X/Fe] versus [Fe/H] for the program stars. For the bottom panel, α is the average of O, Si, Ca, and Ti. Thin disc (open aqua circles), thick disc (filled blue circles), and bulge (red triangles) red giant stars from Alves-Brito et al. (2010) are overplotted in each panel. The thick-disc comparison star HD 40409 is located at [Fe/H] = +0.20 and includes an error bar.

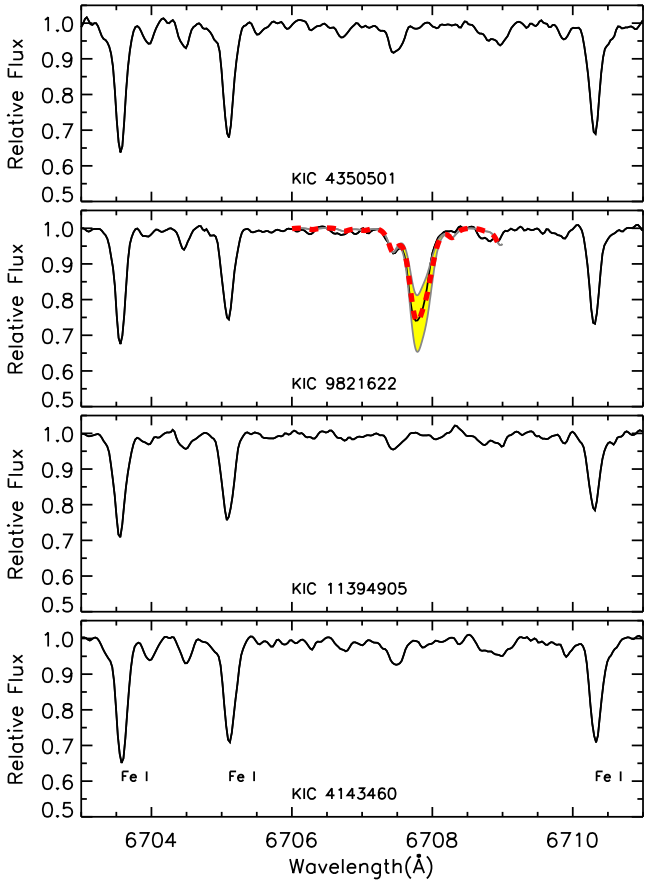

Figure 2. Spectra near the 6707.8 Å Li line for the program stars. In the second panel, we overplot the best-fitting synthetic spectra (red dashed lines) corresponding to $A(Li)_{NLTE} = 1.76$. The shaded yellow region corresponds to synthetic spectra which differ from the best fit by $\pm$ 0.2 dex. The spectra were corrected for their heliocentric radial velocity and the locations of some nearby Fe I lines are indicated in the lower panel.

comparison sample. The program stars occupy the same region of chemical abundance space as the comparison thin disc, thick disc, and bulge objects. It is not obvious, however, whether the program stars more closely follow the thin disc or thick disc abundance trends due to the different behaviour of the four α-elements. Nevertheless, based on these α-elements, we conclude that there are no unusual chemical abundance patterns amongst the program stars.

Our analysis also included the Fe-peak elements Cr, Ni, and Cu. For these elements, the program stars lie on, or very near, the well-defined trends exhibited by local red giant stars of comparable metallicity (e.g. Luck & Heiter 2007). Unlike the α-elements, however, the possibility exists that there may be systematic abundance offsets between our values and the literature comparison sample for these three elements as we have no stars in common.

We measured abundances for the neutron-capture elements Ba, La, and Eu. The first two elements are produced primarily through the *s*-process while the latter is an *r*-process element. Observations of open cluster giants indicate that the Ba abundance increases with decreasing age (D'Orazi et al. 2009). Such a chemical signature was interpreted as being due to extra contributions from low-mass stars to the Galactic chemical evolution. Abundance trends with age, however, are not seen for other *s*-process elements such as Zr and La (Jacobson & Friel 2013). We find [Ba/Fe] $\lesssim$ 0.15 and in the context of the D'Orazi et al. (2009) results, the program stars resemble open clusters with ages > 2 Gyr. Within our limited sample, however, the [Ba/Fe] ratio appears to *decrease* with increasing mass. Assuming mass is a proxy for age, then this trend between abundance and age would be opposite to that seen among the open clusters. More data are needed to examine this intriguing result. The program stars all have enhanced [Eu/Fe] ratios, and high ratios would be expected given that Eu and the α-elements typically follow each other (e.g. Woolf, Tomkin & Lambert 1995; Sakari et al. 2011). That said, the [Eu/Fe] ratios are slightly higher than [α/Fe], although the former are based on a single line.

Finally, we measured lithium abundances (or limits) for the program stars using spectrum synthesis (see Fig. 2). Only KIC 9821622 (J19083615+4641212) has a detectable 6707 Å lithium line and we measure $A(Li)_{LTE} = 1.63$ and $A(Li)_{NLTE} = 1.76$ using the NLTE corrections from Lind, Asplund & Barklem (2009). While this star appears to be lithium rich when compared to the other program stars,

the degree of enrichment is considerably smaller than the highest values found in some giant stars, $A(Li)_{LTE} \simeq 4$ (Reddy & Lambert 2005). For the other three stars, the lithium abundance limits, $A(Li)_{LTE} \lesssim 0.4$, overlap with the limits in giant stars presented by Luck & Heiter (2007).

Jofré et al. (2015) also studied KIC 9821622 using the GRACES spectra available at the Gemini web site (recall that our analysis is based on spectra from an updated version of the OPERA data reduction pipeline). With the exception of $T_{\rm eff}$, their stellar parameters $T_{\rm eff}/\log g/\xi_t/[{\rm Fe/H}] = 4725/2.73/1.12/-0.49$ are in fair agreement with ours values $T_{\rm eff}/\log g/\xi_t/[{\rm Fe/H}] = 4895/2.71/1.17/-0.40$. For $T_{\rm eff}$, the difference is 170K; their values are derived from excitation equilibrium of Fe I lines while we employed the IR flux method. For the elements in common between the two studies (Li, O, Si, Ca, Ti, Cr, Fe, Ni, Ba, La, and Eu), the abundance ratios are in good agreement with a mean difference of 0.00 ± 0.05 dex ($\sigma = 0.17$). All elements agree to within 0.20 dex between the two studies with the exception of O and Si for which the differences in [X/Fe] are 0.38 and 0.24 dex, respectively. Stellar parameters ($T_{\rm eff}$), line selection, and/or atomic data are the likely causes of the abundance differences.

4 DISCUSSION

4.1 Chemical abundances

All chemical abundance ratios appear 'normal' when compared to local red giant stars of similar metallicity. That is, our program stars exhibit no unusual chemical abundance signatures that could provide clues to the origin of these unusually massive and young stars with enhanced [α/Fe] ratios. (We will return to the lithium-rich object later in the discussion.) Given the chemical similarities between local thick disc stars and those of the inner disc, and bulge (Alves-Brito et al. 2010; Bensby et al. 2010), it is difficult to use chemical abundances to test the scenario proposed by Chiappini et al. (2015) in which these young [α/Fe]-rich objects were formed near the Galactic bar and migrated to their current locations.

4.2 Line broadening

Line broadening offers another possible clue to the origin of the program stars. In particular, high line broadening could arise as the result of mass transfer and/or stellar mergers and these processes are relevant in the context of the blue straggler explanation proposed by Martig et al. (2015). We note that the APOGEE pipeline does not measure broadening. We measured the line broadening from spectrum synthesis and χ^2 minimization for five lines (Cu I 5105.50 Å, Cu I 5782.14 Å, Ba II 5853.69 Å, Ba II 6141.73 Å, Ba II 6496.91 Å). These lines were already used in our abundance analysis and are not too weak, nor too strong, such that reliable measurements should be obtained. The broadening values[6] spanned a narrow range from 7.0 ± 0.4 km s^{-1} (KIC 4350501) to 7.7 ± 0.2 km s^{-1}(KIC 11394905). For a given star, the broadening values from the five atomic lines were in very good agreement. We emphasize that our measurements were obtained by fitting a single Gaussian function which incorporates the (i) instrumental profile, (ii) rotation, and (iii) macroturbulent velocity. For the GRACES spectra, the instrumental broadening alone accounts for 4.4 km s^{-1} and thus the combined macroturbulent velocity and rotational broadening ranges from 5.5 to 6.3 km s^{-1}, and such values appear normal for giant stars (Carney et al. 2003; Hekker & Meléndez 2007; Luck & Heiter 2007). Therefore, none of the program stars appear to be unusually broad lined.

[6] These values are the full width at half-maximum of a Gaussian function applied to the synthetic spectra and the line list includes IS, hfs, and blends.

Table 7. Heliocentric radial velocities (km s^{-1}).

Name	Date	RV	σRV	APOGEE
KIC 4350501	4 Jun 2015	−83.4	0.5	−83.3
KIC 9821622	21 Jul 2015	−6.0	0.4	−5.5
KIC 11394905	21 Jul 2015	−69.8	0.5	−75.5
KIC 4143460	21 Jul 2015	+6.6	0.5	+6.6

4.3 Radial velocities and kinematics

As noted by Martig et al. (2015), these young [α/Fe]-rich stars do not possess unusual kinematic properties when compared to the other [α/Fe]-rich objects. We measured heliocentric radial velocities from the observed wavelengths of the lines used in the EW analysis (see Table 7). For three stars (KIC 4350501, KIC 9821622, and KIC 4143460), our measured radial velocities are in excellent agreement with the APOGEE values, i.e. these stars exhibit no evidence for radial velocity variation beyond ∼1 km s^{-1}.

For one star, KIC 11394905, there is evidence for a ∼6 km s^{-1} radial velocity variation between the APOGEE and GRACES spectra, suggesting the presence of at least one binary in our sample. In the context of the blue straggler origin, the binary fraction offers a key diagnostic (e.g. Brogaard et al. 2016). Based on radial velocity monitoring of the M67 open cluster, the blue straggler binary frequency is 79 ± 24 per cent which is significantly higher than the binary frequency of 22.7 ± 2.1 per cent for the remaining M67 objects (Geller, Latham & Mathieu 2015). Radial velocity measurements of metal-poor field blue stragglers also reveal a high binary fraction of 47 ± 10 per cent (Carney et al. 2001); the same group find a binary fraction of ∼16 per cent among 'normal' metal-poor stars (Carney et al. 2003).

Martig et al. (2015) dismissed the blue straggler origin on the following grounds. They estimated the number of evolved blue stragglers to be a factor of 3–4 lower than the young [α/Fe]-rich stars in their sample. That said, there are selection biases for the *Kepler* sample as well as for the subset observed by APOGEE that need to be taken into account. Additionally, Martig et al. (2015) found no evidence for anomalous surface rotation which some blue stragglers possess. Finally, they noted that the radial velocity variation among the APOGEE spectra for individual stars was small, $\sigma{\rm RV} < 0.2$ km s^{-1}.

For the four program stars, however, only two (KIC 4350501 and KIC 4143460) have multiple radial velocity measurements from APOGEE; both have three measurements with a baseline of ∼30 d. Given that metal-poor blue stragglers tend to have long periods, > 100 d, and semi-amplitudes of ∼10 km s^{-1} (Carney et al. 2001), we suggest that it is unlikely that APOGEE would have detected radial velocity variations, if present, over such a short baseline.

Combining the APOGEE radial velocities with those measured from the GRACES spectra, we now have additional epochs and a longer baseline over which to examine the likelihood of detecting radial velocity variation. Following Norris et al. (2013), we can then ask the following question: what is the probability of observing a

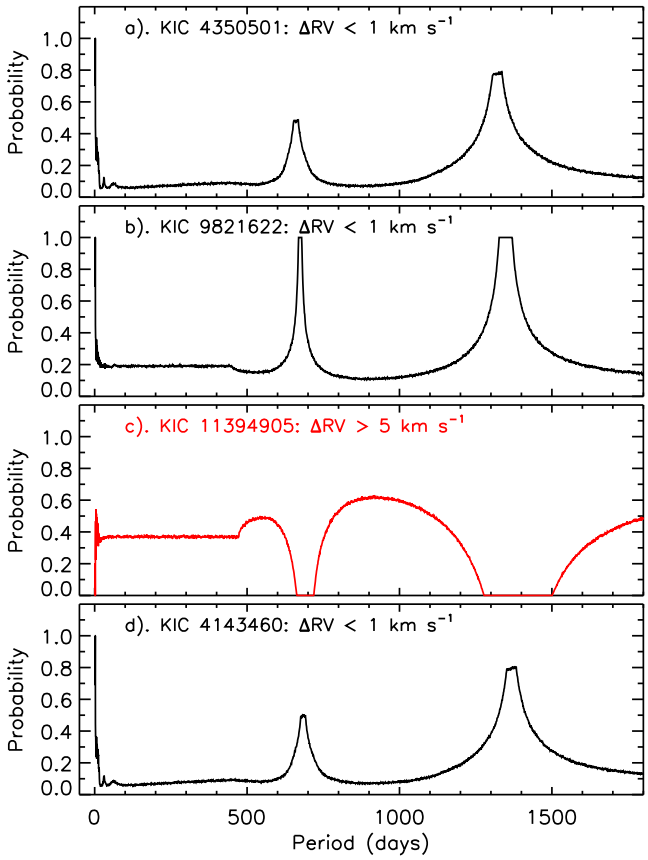

Figure 3. Probability of detecting radial velocity amplitudes $\leq$1 km s^{-1} (panels a, b, and d) or $\geq$5 km s^{-1} (panel c) as a function of period for the program stars. These values were based on Monte Carlo simulations assuming a semi-amplitude of 10 km s^{-1}, circular orbits, the observed number of epochs and their time spans (see text for details). The peaks in probability correspond to the differences in dates when the stars were observed by APOGEE and GRACES.

radial velocity variation ≤ 1.0[7] km s^{-1} given the observed number of epochs and their time spans? Using Monte Carlo simulations, we estimated these probabilities in the following way. We assumed that each star had a circular orbit with a semi-amplitude of 10 km s^{-1}; such values appear typical for blue stragglers (Carney et al. 2001). We tested all periods from 0.5 to 30 d (in steps of 0.5 d) and then from 30 to 1800 d (in steps of 1 d). For a given assumed period, we performed 10 000 realizations in which the inclination angle was randomly set and the first 'observation' was set at a random phase. For all epochs of observation, we could obtain velocities. We then asked the question: for what fraction of realizations is the maximum velocity difference $\leq$1.0 km s^{-1}? We plot those results in panels a, b, and d in Fig. 3. Given the small number of radial velocity measurements, we cannot exclude the possibility that these stars are binaries. The high probability peaks near 700 and 1350 d are caused by the typical baseline between the first APOGEE measurements and the GRACES observations.

For KIC 11394905 (panel c in Fig. 3), the two radial velocity measurements differ by $\sim$6 km s^{-1} and we asked a slightly different question: for what fraction of realizations is the maximum velocity difference $\geq$5.0[8] km s^{-1}? The limited observations can only preclude periods around 700 and 1400 d.

Informed by the above simulations, we conclude that all program stars could be evolved blue stragglers and we do not have sufficient radial velocity measurements to exclude binarity. Therefore, long-term radial velocity monitoring for the entire sample from Martig et al. (2015) is essential to establish any radial velocity variation and thereby place stronger constraints on the blue straggler hypothesis.

Preston & Sneden (2000) found no evidence for *s*-process enhancements among their sample of long period low eccentricity blue stragglers. Similarly, our sample also exhibit no evidence for *s*-process element enrichment.

Finally, recall that one star, KIC 9821622, appears to be lithium rich. The exact process that causes enhanced Li abundances in a small fraction of evolved stars has not been identified (e.g. Charbonnel & Balachandran 2000), and the heterogeneity in evolutionary phase among Li-rich giants suggests that multiple mechanisms may be at work (Martell & Shetrone 2013). If our sample are evolved blue stragglers, then the mechanism(s) responsible for lithium enrichment must also operate in these objects.

4.4 Spectral energy distributions

To further explore the possibility that these stars could be blue stragglers, or binaries in general, we examine their spectral energy distributions (SEDs). To reiterate, the key aspect we are focusing upon is the possibility that the program stars are binaries such that the inferred masses are high due to mass transfer or merger leading to ages that are underestimated for a single star. SEDs were created using the Spanish Virtual Observatory SED Analyzer (VOSA)[9] (Bayo et al. 2008). For the program stars, the SEDs are generated using photometry from SDSS DR9 (Ahn et al. 2012), Tycho-2 (Høg et al. 2000), 2MASS (Majewski et al. 2003), and *WISE* (Wright et al. 2010) and fit using the BT-NextGen (AGSS2009) grid of stellar model atmospheres created by Allard, Homeier & Freytag (2012). (For 4350501, the 22 μm *WISE* W4 bandpass was not included in the fit.) In Fig. 4, we find that two stars (KIC 9821622 and KIC 4350501) exhibit an IR excess and a third star (KIC 4143460) may also show an IR excess. The IR excess is most notable in the 22 μm *WISE* W4 bandpass.

Among red giant stars, <1 per cent exhibit an IR excess (Jones 2008; Bharat Kumar et al. 2015). On the other hand, IR excesses are commonly found in post-asymptotic giant branch, RV Tauri, and Lambda Bootis stars (e.g. Van Winckel, Waelkens & Waters 1995; Giridhar et al. 2005). These objects are (likely) binary systems with debris discs or dusty circumstellar environments that have undergone dust–gas winnowing (see Venn et al. 2014). An examination of all 14 stars in the Martig et al. (2015) sample show that only five stars have clear IR excesses, including three of these stars with GRACES spectra.

[7] For three of the four program stars, the differences in radial velocities between APOGEE and GRACES are below 1 km s^{-1}. While the uncertainties in the APOGEE and GRACES radial velocities are $\sim$ 0.5 km s^{-1}, we do not know for certain whether the zero-points are the same. We therefore conservatively adopt a threshold velocity difference of 1 km s^{-1} when exploring the current observational constraints on binarity.

[8] Again, we do not know whether the APOGEE and GRACES measurements have the same zero-points, so we conservatively adopt a threshold value of 5 km s^{-1} in this exercise.

[9] http://svo2.cab.inta-csic.es/theory/vosa/

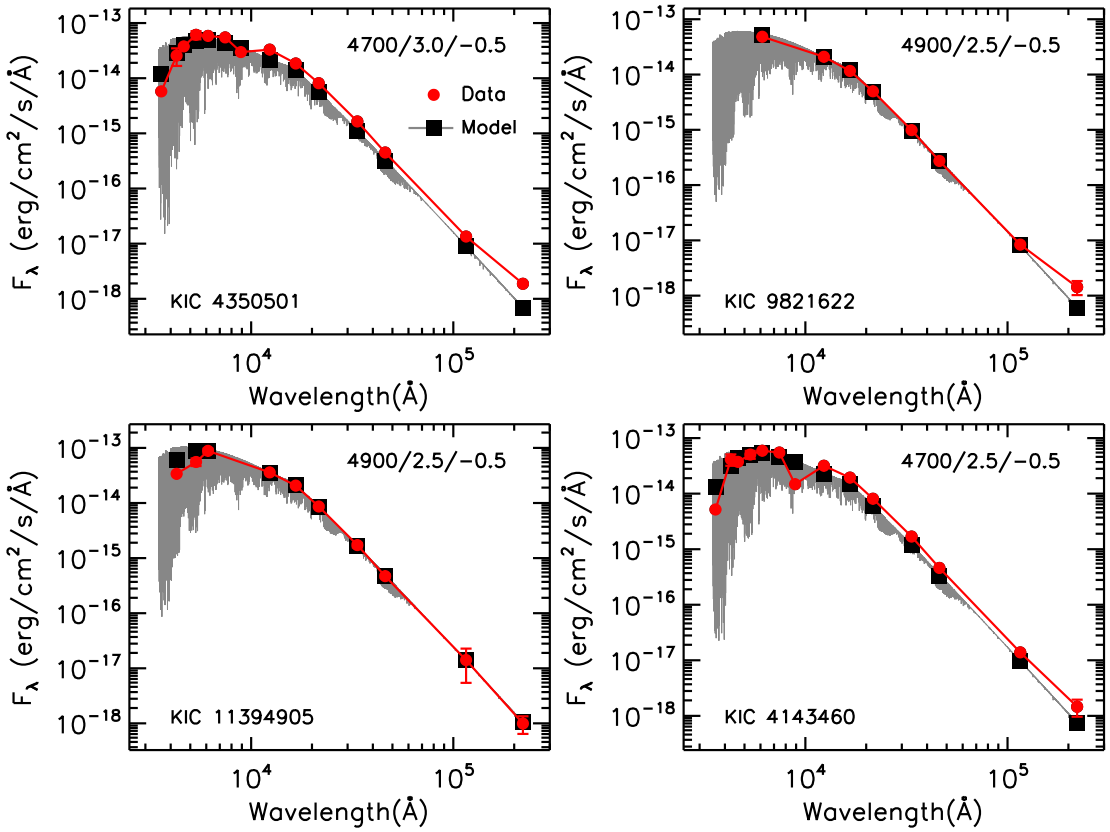

Figure 4. SEDs for the four program stars (red circles). The best-fitting models (black squares) and theoretical spectra (grey lines) are overplotted. The model parameters ($T_{\rm eff}$/log g/[Fe/H]) are indicated in each panel. (See text for details on the SEDs and the fitting.)

5 CONCLUSIONS

We have analysed high-resolution spectra of four massive (i.e. young) [α/Fe]-rich stars from Martig et al. (2015) obtained using Gemini-GRACES during the 2015 on-sky tests. While one object appears to be lithium rich, we find no chemical abundance anomalies among the program stars when compared to local giants. Although only one of the four stars exhibits a radial velocity variation, given the small number of radial velocity measurements, we cannot exclude the possibility that the three remaining stars are binaries. Martig et al. (2015) suggested that these young [α/Fe]-rich stars could be evolved blue stragglers. The SEDs indicate that two (and perhaps three) of the four stars exhibit an IR excess, characteristic of certain types of binary stars. In light of the high $>$ 50 per cent binary fraction among blue stragglers, long-term radial velocity monitoring is essential to test this scenario.

ACKNOWLEDGEMENTS

This work is based on observations obtained with ESPaDOnS, located at the Canada–France–Hawaii Telescope (CFHT). CFHT is operated by the National Research Council of Canada, the Institut National des Sciences de l'Univers of the Centre National de la Recherche Scientique of France, and the University of Hawai'i. ESPaDOnS is a collaborative project funded by France (CNRS, MENESR, OMP, LATT), Canada (NSERC), CFHT, and ESA. ESPaDOnS was remotely controlled from the Gemini Observatory, which is operated by the Association of Universities for Research in Astronomy, Inc., under a cooperative agreement with the NSF on behalf of the Gemini partnership: the National Science Foundation (United States), the National Research Council (Canada), CONICYT (Chile), the Australian Research Council (Australia), Ministério da Ciência, Tecnologia e Inovação (Brazil), and Ministerio de Ciencia, Tecnología e Innovación Productiva (Argentina). We thank the anonymous referee for helpful comments. DY thanks John E. Norris for helpful discussions. DY, LC, MA, AD, and KS gratefully acknowledge support from the Australian Research Council (grants FL110100012, DP120100991, FT140100554, and DP150100250). SM gratefully acknowledges support from the Australian Research Council (grant DE 140100598). JM thanks support by FAPESP (2010/50930-6).

REFERENCES

Ahn C. P. et al., 2012, ApJS, 203, 21
Allard F., Homeier D., Freytag B., 2012, Phil. Trans. R. Soc. A, 370, 2765
Alves-Brito A., Meléndez J., Asplund M., Ramírez I., Yong D., 2010, A&A, 513, A35
Amarsi A. M., Asplund M., Collet R., Leenaarts J., 2015, MNRAS, 454, L11
Asplund M., Grevesse N., Sauval A. J., Scott P., 2009, ARA&A, 47, 481
Baglin A. et al., 2006, 36th COSPAR Scientific Assembly. p. 3749
Barklem P. S., Aspelund-Johansson J., 2005, A&A, 435, 373
Barklem P. S., Piskunov N., O'Mara B. J., 2000, A&AS, 142, 467
Bayo A., Rodrigo C., Barrado Y., Navascués D., Solano E., Gutiérrez R., Morales-Calderón M., Allard F., 2008, A&A, 492, 277
Bensby T., Alves-Brito A., Oey M. S., Yong D., Meléndez J., 2010, A&A, 516, L13
Bensby T., Feltzing S., Oey M. S., 2014, A&A, 562, A71
Bharat Kumar Y., Reddy B. E., Muthumariappan C., Zhao G., 2015, A&A, 577, A10

Blackwell D. E., Ibbetson P. A., Petford A. D., Shallis M. J., 1979a, MNRAS, 186, 633
Blackwell D. E., Petford A. D., Shallis M. J., 1979b, MNRAS, 186, 657
Blackwell D. E., Petford A. D., Shallis M. J., Simmons G. J., 1980, MNRAS, 191, 445
Blackwell D. E., Booth A. J., Haddock D. J., Petford A. D., Leggett S. K., 1986, MNRAS, 220, 549
Blackwell D. E., Lynas-Gray A. E., Smith G., 1995, A&A, 296, 217
Brogaard K. et al., 2016, Astron. Nachr., preprint (arXiv:1601.01412)
Brown T. M., Gilliland R. L., Noyes R. W., Ramsey L. W., 1991, ApJ, 368, 599
Carney B. W., Latham D. W., Laird J. B., Grant C. E., Morse J. A., 2001, AJ, 122, 3419
Carney B. W., Latham D. W., Stefanik R. P., Laird J. B., Morse J. A., 2003, AJ, 125, 293
Casagrande L., Ramírez I., Meléndez J., Bessell M., Asplund M., 2010, A&A, 512, A54
Casagrande L. et al., 2014, ApJ, 787, 110
Casagrande L. et al., 2016, MNRAS, 455, 987
Castelli F., Kurucz R. L., 2003, in Piskunov N., Weiss W. W., Gray D. F., eds, Proc. IAU Symp. 210, Modelling of Stellar Atmospheres. Uppsala, Sweden, p. 20P
Chaplin W. J., Miglio A., 2013, ARA&A, 51, 353
Chaplin W. J. et al., 2014, ApJS, 210, 1
Charbonnel C., Balachandran S. C., 2000, A&A, 359, 563
Chené A.-N. et al., 2014, in Navarro R., Cunningham C. R., Barto A. A., eds, Proc. SPIE Conf. Ser. Vol. 9151, Advances in Optical and Mechanical Technologies for Telescopes and Instrumentation. SPIE, Bellingham, p. 915130
Chiappini C. et al., 2015, A&A, 576, L12
Cunha K., Sellgren K., Smith V. V., Ramirez S. V., Blum R. D., Terndrup D. M., 2007, ApJ, 669, 1011
D'Orazi V., Magrini L., Randich S., Galli D., Busso M., Sestito P., 2009, ApJ, 693, L31
Donati J.-F., 2003, in Trujillo-Bueno J., Sanchez Almeida J., eds, ASP Conf. Ser. Vol. 307, Solar Polarization. Astron. Soc. Pac., San Francisco, p. 41
Dotter A., Chaboyer B., Jevremović D., Kostov V., Baron E., Ferguson J. W., 2008, ApJS, 178, 89
Epstein C. R. et al., 2014, ApJ, 785, L28
Fuhr J. R., Wiese W. L., 2006, J. Phys. Chem. Ref. Data, 35, 1669
Fuhrmann K., 2011, MNRAS, 414, 2893
García Pérez A. E. et al., 2015, AJ, preprint (arXiv:1510.07635)
Geller A. M., Latham D. W., Mathieu R. D., 2015, AJ, 150, 97
Gilliland R. L. et al., 2010, PASP, 122, 131
Giridhar S., Lambert D. L., Reddy B. E., Gonzalez G., Yong D., 2005, ApJ, 627, 432
Gratton R. G., Carretta E., Claudi R., Lucatello S., Barbieri M., 2003, A&A, 404, 187
Hekker S., Meléndez J., 2007, A&A, 475, 1003
Høg E. et al., 2000, A&A, 355, L27
Ivans I. I., Kraft R. P., Sneden C., Smith G. H., Rich R. M., Shetrone M., 2001, AJ, 122, 1438
Ivans I. I., Simmerer J., Sneden C., Lawler J. E., Cowan J. J., Gallino R., Bisterzo S., 2006, ApJ, 645, 613
Jacobson H. R., Friel E. D., 2013, AJ, 145, 107
Jofré E., Petrucci R., García L., Gómez M., 2015, A&A, 584, L3
Jones M. H., 2008, MNRAS, 387, 845
Kobayashi C., Nakasato N., 2011, ApJ, 729, 16
Kurucz R., 1993, ATLAS9 Stellar Atmosphere Programs and 2 km/s grid. Kurucz CD-ROM No. 13. Smithsonian Astrophysical Observatory, Cambridge
Kurucz R. L., Bell B., 1995, Atomic Line List. Smithsonian Astrophysical Observatory, Cambridge
Lawler J. E., Bonvallet G., Sneden C., 2001a, ApJ, 556, 452
Lawler J. E., Wickliffe M. E., den Hartog E. A., Sneden C., 2001b, ApJ, 563, 1075
Lebreton Y., Goupil M. J., 2014, A&A, 569, A21
Lind K., Asplund M., Barklem P. S., 2009, A&A, 503, 541
Luck R. E., Heiter U., 2007, AJ, 133, 2464
McWilliam A., 1998, AJ, 115, 1640
Majewski S. R., Skrutskie M. F., Weinberg M. D., Ostheimer J. C., 2003, ApJ, 599, 1082
Majewski S. R. et al., 2015, AJ, preprint (arXiv:1509.05420)
Martell S. L., Shetrone M. D., 2013, MNRAS, 430, 611
Martig M. et al., 2015, MNRAS, 451, 2230
Martioli E., Teeple D., Manset N., Devost D., Withington K., Venne A., Tannock M., 2012, in Radziwill N. M., Chiozzi G., eds, Proc. SPIE Conf. Ser. Vol. 8451, Software and Cyberinfrastructure for Astronomy II. SPIE, Bellingham, p. 84512B
Matteucci F., Greggio L., 1986, A&A, 154, 279
Mészáros S. et al., 2012, AJ, 144, 120
Miglio A. et al., 2013a, in EPJ Web Conf., 43, 03004
Miglio A. et al., 2013b, MNRAS, 429, 423
Nissen P. E., 2015, A&A, 579, A52
Norris J. E. et al., 2013, ApJ, 762, 28
Pinsonneault M. H. et al., 2014, ApJS, 215, 19
Preston G. W., Sneden C., 2000, AJ, 120, 1014
Prochaska J. X., Naumov S. O., Carney B. W., McWilliam A., Wolfe A. M., 2000, AJ, 120, 2513
Ramírez S. V., Cohen J. G., 2002, AJ, 123, 3277
Reddy B. E., Lambert D. L., 2005, AJ, 129, 2831
Sakari C. M., Venn K. A., Irwin M., Aoki W., Arimoto N., Dotter A., 2011, ApJ, 740, 106
Sills A., Karakas A., Lattanzio J., 2009, ApJ, 692, 1411
Silva Aguirre V. et al., 2013, ApJ, 769, 141
Silva Aguirre V. et al., 2015, MNRAS, 452, 2127
Sneden C., 1973, ApJ, 184, 839
Sobeck J. S. et al., 2011, AJ, 141, 175
Stetson P. B., Pancino E., 2008, PASP, 120, 1332
Tinsley B. M., 1979, ApJ, 229, 1046
Ulrich R. K., 1986, ApJ, 306, L37
Unsöld A., 1955, Physik der Sternatmospharen, MIT besonderer Berucksichtigung der Sonne. Springer-Verlag, Berlin
Van Winckel H., Waelkens C., Waters L. B. F. M., 1995, A&A, 293, L25
Venn K. A., Irwin M., Shetrone M. D., Tout C. A., Hill V., Tolstoy E., 2004, AJ, 128, 1177
Venn K. A., Puzia T. H., Divell M., Côté S., Lambert D. L., Starkenburg E., 2014, ApJ, 791, 98
Woolf V. M., Tomkin J., Lambert D. L., 1995, ApJ, 453, 660
Wright E. L. et al., 2010, AJ, 140, 1868
Yong D., Grundahl F., Nissen P. E., Jensen H. R., Lambert D. L., 2005, A&A, 438, 875
Yong D. et al., 2014, MNRAS, 441, 3396

SUPPORTING INFORMATION

Additional Supporting Information may be found in the online version of this article:

Table 3. Line list for the program stars.
Table 6. Abundance errors from uncertainties in atmospheric parameters.
(http://www.mnras.oxfordjournals.org/lookup/suppl/doi:10.1093/mnras/stw676/-/DC1).

Please note: Oxford University Press is not responsible for the content or functionality of any supporting materials supplied by the authors. Any queries (other than missing material) should be directed to the corresponding author for the article.

This paper has been typeset from a TEX/LATEX file prepared by the author.